

Short Communication

Comparison of Defects in Hydride Vapor Phase Epitaxy-Grown GaN Films under Different V/III Ratios and the Influence on the Electrical and Optical Properties

Y. Tian^{#1,3,4}, R.S. Wei^{#2}, Y.L. Shao^{1,*}, X.P. Hao¹, Y.Z. Wu¹, L. Zhang¹, Y.B. Dai¹, Q. Huo¹, B.G. Zhang¹, H.X. Hu¹

¹ State Key Lab of Crystal Materials, Shandong University, Jinan, 250100, PR China

² Shanxi Semicore Crystal Co., Ltd., Taiyuan, 030024, PR China

³ Key Lab of Advanced Transducers and Intelligent Control System, Ministry of Education and Shanxi Province, Taiyuan University of Technology, Taiyuan, 030024, PR China

⁴ College of Physics and Optoelectronics, Taiyuan University of Technology, Taiyuan, 030024, PR China

*E-mail: ylshao@sdu.edu.cn

[#] Y. Tian and R.S. Wei are co-first authors of the article.

Received: 4 August 2020 / Accepted: 22 September 2020 / Published: 31 October 2020

In this paper, GaN films were grown by hydride vapor phase epitaxy under different ratios of NH₃ to GaCl (V/III ratio). Secondary ion mass spectrometry measurements of [Si], [O], [C] and [H] were carried out to analyse the changes in impurities. Molten KOH - NaOH eutectic etching was applied to reveal changes in the dislocation density. With increasing V/III ratio, [O] and the dislocation density decrease, while [Si] increases. Further the influence of the V/III ratio on the electrical and optical properties was examined by Hall and photoluminescence measurements.

Keywords: GaN, Defects, V/III Ratios, Electrical properties, Optical properties

1. INTRODUCTION

Recently, GaN has been widely used in optoelectronic and microelectronic devices such as ultraviolet and blue light-emitting diodes, visible-blind detectors, lasers and high frequency field effect transistors [1, 2]. However, due to the shortage of GaN crystal substrates, the electrical and optical properties of devices are seriously hindered. Hydride vapor phase epitaxy (HVPE) is the main method for GaN crystal growth and has the advantages of low cost, simplicity and rapid growth speed [3]. GaN bulk is grown on a c-oriented Al₂O₃ substrate in most cases. For device applications, both impurities and dislocations are crucial factors because they directly influence the concentration and mobility of

carriers as well as the optical properties. The V/III ratio has a strong influence on the quality and properties of GaN [4]. Several researchers have reported the growth and properties of GaN with different V/III ratios. In GaN grown by MBE, the point defect density, morphology and electrical properties are strongly dependent on the growth stoichiometry [5]. The oxygen and Ga vacancy concentrations increase with decreasing Ga/N ratio. Meanwhile, the electron mobility improves. In metal organic chemical vapor deposition (MOCVD)-grown GaN, the V/III ratio should be slightly larger than the desorption rates of N/Ga to acquire high-quality GaN. The yellow emission decreases with increasing V/III ratio [6]. To our knowledge, there is no systematic study of the effect of V/III on defects in HVPE GaN. Here, we report the impurities and dislocations of GaN grown by HVPE under different V/III ratios. Further analyses of how the defects impact the electrical and optical properties were performed.

2. EXPERIMENTAL

Three GaN films were prepared on 2 inch c-oriented Al₂O₃ substrates with 3 µm MOCVD GaN. The substrates were commercially purchased. The dislocation density of the MOCVD GaN layers was $\sim 3 \times 10^8 \text{ cm}^{-2}$, and the surface was quite smooth under SEM at 1000 magnification. GaN films were grown in a homemade vertical HVPE reactor. The wall of the reactor was a quartz tube with a 4 inch diameter. The HVPE system contained two zones (the source zone and the deposition zone) with different temperatures. In the source zone, HCl gas reacted with liquid Ga to form GaCl. Then, GaCl was transported to the deposition zone, where it reacted with NH₃ to form GaN. N₂ was used as the carrier gas. GaN films were grown at atmospheric pressure. For the GaN samples, the only difference was the V/III ratio, which was 10, 20 or 50. Table 1 shows the growth parameters of the GaN films. The growth rate was proportional to the HCl flow (100 µm/h at V/III=10, 50 µm/h at V/III=20, and 20 µm/h at V/III=50). The thickness of all GaN films was 100 µm.

Table 1. Growth parameters of GaN.

Growth parameters	V/III=1	V/III=2	V/III=5
	0	0	0
HCl (sccm)	100	50	20
NH ₃ (sccm)	1000	1000	1000
source zone (°C)	820	820	820
deposition zone (°C)	1050	1050	1050

Secondary ion mass spectrometry (SIMS, by EVANS) was adopted to study the impurity concentration. A Hall effect measurement system (Accent HL5500) was employed to characterize the electron concentration and mobility. Photoluminescence (PL) measurements were used to detect the optical properties. The excitation source was a 325 nm He–Cd laser.

3. RESULTS AND DISCUSSION

Microscope images of GaN films under different V/III with a magnification of 100 are shown in Fig. 1. When the V/III ratio is 10, the steps are very obvious, and the GaN film has few cracks; when the V/III ratio increases to 20, the steps decrease, the surface flatness improves, and a few cracks appear. When the V/III ratio increases to 50, the steps disappear, and the surface becomes quite smooth. Meanwhile, cracks increase obviously.



Figure 1. Microscope images of GaN grown at (a) V/III=10, (b) V/III=20, and (c) V/III=50.

Fig. 2 depicts the SIMS result of GaN grown under different V/III ratios. As the V/III ratio increases from 10 to 20 to 50, [Si] increases from $2.2 \times 10^{16} \text{ cm}^{-3}$ to $3.5 \times 10^{16} \text{ cm}^{-3}$ to $4.4 \times 10^{16} \text{ cm}^{-3}$; [O] decreases from $2.4 \times 10^{17} \text{ cm}^{-3}$ to $1.8 \times 10^{17} \text{ cm}^{-3}$ to $1.5 \times 10^{17} \text{ cm}^{-3}$; [C] decreases from $6.4 \times 10^{16} \text{ cm}^{-3}$ to $3.8 \times 10^{16} \text{ cm}^{-3}$ and then increases to $7.1 \times 10^{16} \text{ cm}^{-3}$; and [H] is almost invariant. The quartz subassembly is the main source of silicon. As the formation energy of Si_{Ga} is very low, all Si in gas is incorporated into Ga sites. [7] The growth rate of GaN decreases with increasing V/III, and the growth time increases with increasing V/III. Hence, more Si is incorporated into the gas, which induces an increase in silicon impurities. The sources of oxygen in the HVPE system include the (i) quartz subassembly, (ii) background vacuum pressure, (iii) water impurity of water, and (iv) Ga source [8]. An increase in GaCl can suppress the volatility of Ga_2O_3 . Hence, the oxygen content increases with decreasing V/III ratio. Carbon mainly comes from the graphite substrate holder. For unintentional n-type GaN, C_{N} is the most favoured configuration for the carbon impurity when present as an unintentional impurity. [9] The content of C is affected by a decrease in the growth rate and an increase in N vacancies. When the V/III ratio is small, it is easy for C to incorporate on N sites. An increase in the V/III ratio reduces the likelihood of the formation of nitrogen vacancies. As the V/III ratio increases, the incorporation of C on N sites becomes difficult, which induces a decrease in the C content. With a further increase in the V/III ratio, N vacancies continue to decrease. However, as the growth rate of GaN decreases, more C is incorporated into the gas. Therefore, the C content becomes larger again when the V/III ratio increases to 50. H mainly comes from NH_3 gas and H_2O in the gas. It acts as an interstitial atom in the GaN film, as the radius of H_2 is very small. In addition, V_{Ga} is an important point defect that can affect the electrical and optical properties. According to our earlier research [3], the V_{Ga} content decreases with increasing V/III ratio.

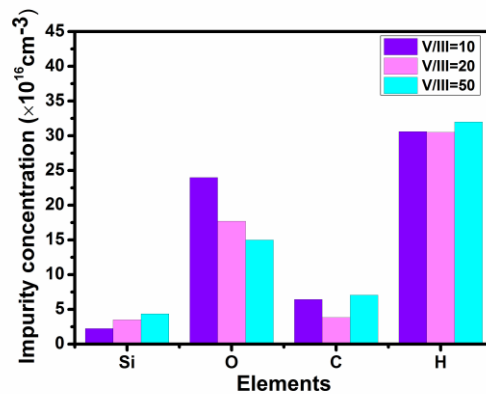


Figure 2. Impurity concentration of GaN grown under different V/III ratios.

Wet chemical etching is a common method to evaluate dislocations with the advantages of simplicity and low cost. To compare the dislocation densities in GaN films, we adopted a eutectic KOH–NaOH (E) mixture to etch GaN films at 450°C for 5 min.[10] Fig. 3 shows SEM images of etched GaN films grown under different V/III ratios. When the V/III ratio is 10, the density of the etching pits is approximately $6.4 \times 10^8 \text{ cm}^{-2}$. When the V/III ratio rises to 20, the density of the etching pits decreases to approximately $2.4 \times 10^8 \text{ cm}^{-2}$. The density of the etching pits changes to approximately $9 \times 10^7 \text{ cm}^{-2}$ when the V/III ratio is 50. According to Dai et al. [3], a large V/III ratio corresponds to a high mobility of Ga and a further rise in the growth speed in the horizontal direction. In contrast, under a small V/III ratio, owing to the short diffusion length of Ga, the 3D growth mode dominates, which leads to a high dislocation density. The dislocations are mainly in the *c* direction, and the orientations of their Burgers vectors are in keeping with **a**, **c** or **a+c**, corresponding to edge dislocations, screw dislocations and mixed dislocations. Although an earlier paper predicted that dislocations had little effect on the electrical properties [11], later calculations indicated that the formation energies of O_N , V_Ga and their complexes are much lower at different positions near threading-edge dislocations than those of the corresponding defects in bulk GaN [12]. The effect of the V/III ratio on dislocations is another factor leading to decreases in the O and V_Ga contents with an increase in the V/III ratio.

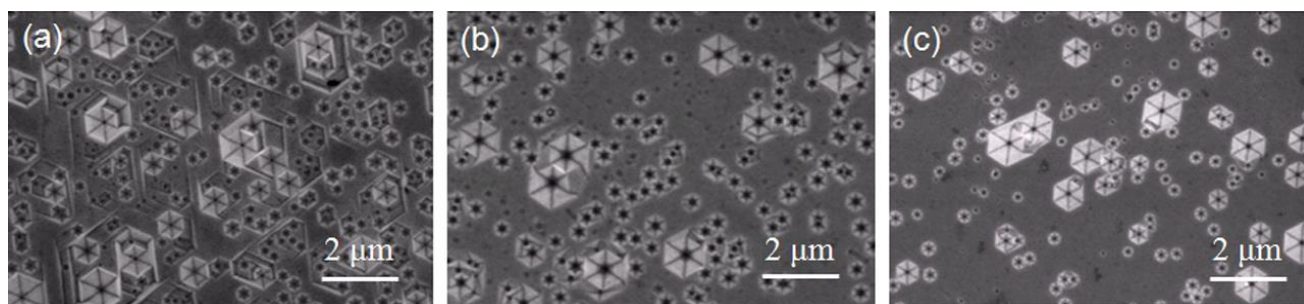


Figure 3. SEM images of E etched films grown at (a) V/III=10, (b) V/III=20, and (c) V/III=50.

Table 2 demonstrates the electron concentration and electron mobility of GaN films under different V/III ratios. According to Table, the electron concentration decreases with increasing V/III

ratio, while the electron mobility increases with increasing V/III ratio. The changing trend of the electron concentration has a close connection with the impurities in GaN films. Silicon acts as a shallow donor in GaN [13] and is widely used as a dopant for n-type GaN. Oxygen is a shallow donor in GaN. According to theoretical and experimental results, oxygen leads to a high free electron concentration of GaN [14,15]. In our experiment, [O] is an order of magnitude larger than [Si]. These concentrations confirm that the high free electron concentration of GaN is due to oxygen. Hydrogen can easily form complexes with other defects in GaN because of the very low formation energy. Hydrogen could be bound to Ga vacancies, forming complexes such as $(V_{\text{Ga}}\text{H})^{2-}$, $(V_{\text{Ga}}\text{H}_2)^-$, $(V_{\text{Ga}}\text{H}_3)$ and $(V_{\text{Ga}}\text{H}_4)^+$ [16]. The isolated hydrogen atom in n-type GaN exists as H^\cdot . The Ga vacancy is negatively charged. There is little chance to form complexes with several H atoms, such as $(V_{\text{Ga}}\text{H}_3)$ and $(V_{\text{Ga}}\text{H}_4)^+$, since H^\cdot will be repelled by the Ga vacancy [17]. As for $(V_{\text{Ga}}\text{H})^{2-}$ and $(V_{\text{Ga}}\text{H}_2)^-$, the calculated energy levels are close to that of the isolated Ga vacancy [16]. V_{Ga} is a well-known acceptor in GaN; hence, an increase in [O] causes an increase in the electron concentration. [18] Based on [O] decreasing with increasing V/III ratio, the electron concentration decreases with increasing V/III ratio.

Table 2. Carrier concentration and electron mobility of GaN grown under different V/III ratios.

V/III	carrier concentration	electron mobility
10	$2.1 \times 10^{18} \text{cm}^{-3}$	$65 \text{ cm}^2/\text{V sec}$
20	$1.1 \times 10^{18} \text{cm}^{-3}$	$209 \text{ cm}^2/\text{V sec}$
50	$7.4 \times 10^{17} \text{cm}^{-3}$	$240 \text{ cm}^2/\text{V sec}$

The electron mobility of GaN can be affected by ionized impurities and dislocations. For an arbitrary degeneracy of the electron gas, the influence of ionized impurity scattering on the mobility is given by [19]

$$\mu = \frac{2^{5.5} \pi}{3} \varepsilon_s^2 \frac{(k_B T)^{1.5} F_3}{N_T q^3 m_n^{0.5} F_1} \quad (1)$$

where

$$F_1 = \int_0^\infty \frac{x^{1/2}}{1 + \exp(x - e_F)} dx$$

$$F_3 = \int_0^\infty \frac{x^3 \exp(x - e_F)}{\phi_i [1 + \exp(x - e_F)]^2} dx$$

$$\phi_i = \ln(1 + \eta) - \frac{\eta}{1 + \eta}$$

$$\eta = \frac{8 m_n \varepsilon_s (k_B T)^2 F_1}{q^2 \hbar^2 n F_2}$$

$$F_2 = \int_0^\infty \frac{x^{1/2} \exp(x - e_F)}{[1 + \exp(x - e_F)]^2} dx$$

$$e_F = \frac{E_F - E_c}{k_B T}$$

ϵ_s is the static dielectric permittivity, k_B is the Boltzmann constant, N_T is the total concentration of ionized impurities, q is the electronic charge, m_n is the electron effective mass, \hbar is the reduced Planck constant, E_c is the bottom of the conduction band, and E_F is the Fermi level. It can be noted from eq. 1 that the mobility limited by ionized impurities follows an inverse relationship with the doping concentration.

Dislocations can also impact the electron mobility. For n-type semiconductors, a dislocation line introduces acceptor centres, which capture electrons from the conduction band [20,21]. The dislocation line becomes negatively charged while a space charge region forms around it. Due to the scattering in the space charge region of electrons traversing it, the mobility decreases. The dislocation line has no scattering effect on electrons traveling parallel to it due to the repulsive potential around the charged dislocation line. The influence of ionized impurity scattering on the mobility in an n-type semiconductor is given by [22]

$$\mu_{dsl} = \frac{\hbar^3 \epsilon_s^2 c^2}{q^3 f^2 m_n^2 N_{dsl} \lambda_D^4} (1 + \varsigma_{\perp})^{3/2} \quad (2)$$

with the Debye length $\lambda_D = \sqrt{\frac{kT \epsilon_s}{q^2 n}}$ describing the screening and the parameter $\varsigma_{\perp} = (2k_{\perp} \lambda_D)^2$ describing the transverse component of the kinetic energy of the electrons. c is the basal lattice constant of wurtzite GaN, f is the occupation rate of the acceptor centres, and N_{dsl} is the dislocation density. According to eq. 2, the mobility limited by dislocations follows an inverse relationship with the dislocation density.

As seen from the SIMS and E etching results, the total impurities first decrease and then remain constant as the V/III ratio increases. Dislocations decrease with increasing V/III ratio. Hence, the electron mobility increases with the V/III ratio.

Fig. 4 depicts the room temperature PL spectra of GaN films under different V/III ratios. The abscissa is the emission wavelength, and the ordinate is the luminous intensity. The band edge emission peak at approximately 362 nm increases and the FWHM of the band edge emission narrows with increasing V/III ratio.

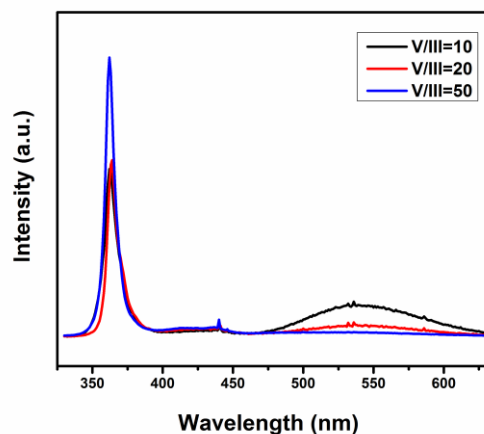


Figure 4. PL spectra of GaN grown under different V/III ratios.

These results indicate that GaN grown under a large V/III ratio has good structural and optical properties. The broad peak at approximately 2.2–2.3 eV is well known as yellow luminescence, which is ubiquitous in n-type GaN. It has been reported that this transition occurs between a shallow donor and a deep acceptor [23,24], and Ga vacancies were suggested to participate in the luminescence transition by acting as deep acceptors [25]. As the Ga vacancy content decreases with increasing V/III ratio, the intensity of yellow luminescence decreases with increasing V/III ratio.

4. CONCLUSIONS

SIMS results reveal the impurity concentration of GaN grown under different V/III ratios. With increasing V/III ratio, [Si] increases while [O] decreases. According to the E etching results, the dislocations decrease as the V/III ratio increases. The changes in defects in different films affect the electrical and optical properties. According to the Hall results, the electron concentration decreases while the electron mobility increases as the V/III ratio increases. According to the PL results, the band edge emission peak becomes stronger while the yellow luminescence band peak becomes weaker as the V/III ratio increases.

ACKNOWLEDGEMENTS

This work was supported by the National Nature Science Foundation of China (Contract No. 51702226, 51572153, 51602177), Natural Science Foundation of Shanxi (Contract No. 201701D221078), and University Science and Technology Innovation Project of Shanxi (Contract No. 201802031).

References

1. O. Akpınar, A. K. Bilgili, M. K. Ozturk, S. Ozcelik and E. Ozbay, *J. Appl. Phys. A*, 125(2) (2019) 112.1-112.13.
2. O. Pohorelec, M. Ľapajna, D. Gregušová, F. Gucmann and J. Kuzmík, *J. Appl. Surf. Sci.*, (2020) 146824.
3. Y. Dai, Y. Shao, Y. Wu, X. Hao, P. Zhang and X. Cao, *J. RSC Adv.*, 4(41) (2014) 21504.
4. G. Koblmüller, F. Reurings, F. Tuomisto and J. S. Speck, *J. Appl. Phys. Lett.*, 97(19) (2010) 191915.
5. D. D. Koleske, A. E. Wickenden, R. L. Henry, W. J. DeSisto and R. J. Gorman, *J. Appl. Phys.*, 84(4) (1998) 1998.
6. H. K. Kim, I. A. Cunningham, Z. Yin, and G. Cho, *J. Prec. Eng. Manuf.*, 9(4) (2008) 86.
7. Van de Walle, G. Chris, C. Stampfl, and J. Neugebauer, *J. Cryst. Growth*, 189-190 (1998) 505.
8. F. Schubert, S. Wirth, F. Zimmermann, J. Heitmann, T. Mikolajick and S. Schmult, *J. Sci. Technol. Adv. Mater.*, 17(1) (2016) 239-243.
9. J. L. Lyons, A. Janotti and d. W. C. G. Van, *J. Phys. Rev.*, 89(3) (2014) 035204.1-035204.8.
10. L. Zhang, Y. Shao, Y. Wu, X. Hao, X. Chen, S. Qu and X. Xu, *J. Alloys Compd.*, 504(1) (2010) 186.
11. J. Elsner, R. Jones, P. K. Sitch, V. D. Porezag, M. Elstner, T. Frauenheim, M. I. Heggie, S. Öberg, and P. R. Briddon, *J. Phys. Rev. Lett.*, 79(19) (1997) 3672.
12. K. X. Chen, Q. Dai, W. Lee, J. K. Kim, E. F. Schubert and Grandusky, *J. Appl. Phys. Lett.*, 93(19) (2008) 192108.
13. R. J. S. Abraham, V. B. Shuman, L. M. Portsel, A. N. Lodygin, Y. A. Astrov and N. V.

- Abrosimov, *J. Phys. Rev.*, 99(19) (2019)195207.1-195207.4.
14. J. Buckeridge, C.R. A. Catlow, D.O. Scanlon, T. W. Keal, P. Sherwood, M. Miskufova, A. Walsh, S. M. Woodley, and A. A. Soko, *J. Phys. Rev. Lett.*, 114 (2015) 016405.
 15. C. Wetzel, T. Suski, J. W. Ager Iii, E. R. Weber, E. E. Haller, S. Fischer, B. K. Meyer, R. J. Molnar, and P. Perlin, *J. Appl. Phys. Lett.* 78(20) (1997) 3923.
 16. B. Gelmont, B. Lund, K. S. Kim, G. U. Jensen, M. Shur and T. A. Fjeldly, *J. Appl. Phys.*, 71(10) (1992) 4977.
 17. C. G. Van de Walle, *Physical Review B*, 56(16) (1997) R10020.
 18. C. G. Van de Walle and J. Neugebauer, *J. Appl. Phys.*, 95(8) (2004) 3851.
 19. B. Gelmont, B. Lund, K. S. Kim, G. U. Jensen, M. Shur, T. A. Fjeldly, *J. Appl. Phys.*, 71(10) (1992) 4977.
 20. W. T. Read Jr, *The London, Edinburgh, and Dublin Philosophical Magazine and Journal of Science*, 45(367) (1954) 775.
 21. V. Kirilyuk, P. R. Hageman, P. C. M. Christianen, W. H. M. Corbeek, M. Zielinski and L. Macht, *J. Physica Status Solidi*, 188(1) (2015) 473-476.
 22. G. L. Pearson, W. T. Read Jr, F. J. Morin, *J. Physical Review*, 93(4) (1954) 666.
 23. M. Julkarnain, T. Fukuda, N. Kamata and Y. Arakawa, *J. Appl. Phys. Lett.*, 107(21) (2015) 100209-848.
 24. A.Y. Polyakov, N.B.Smirnov, E.B.Yakimov, S.A.Tarelkin, A.V.Turutin, I.V.Shemerov, S.J.Pearnton, Kang-Bin Bae and In-HwanLee, *J. Alloys Compd.*, 686 (2016) 1044.
 25. J. Neugebauer and C. G. Van de Walle, *J. Appl. Phys. Lett.*, 69(4) (1996) 503.

© 2020 The Authors. Published by ESG (www.electrochemsci.org). This article is an open access article distributed under the terms and conditions of the Creative Commons Attribution license (<http://creativecommons.org/licenses/by/4.0/>).